

LOW LUMINOSITY GAMMA-RAY BURSTS AS A UNIQUE POPULATION: LUMINOSITY FUNCTION, LOCAL RATE, AND BEAMING FACTOR

ENWEI LIANG^{1,2}, BING ZHANG¹, FRANCISCO VIRGILI¹, Z. G. DAI^{3,1}

¹Department of Physics and Astronomy, University of Nevada, Las Vegas, NV 89154, USA;
 lew@physics.unlv.edu, bzhang@physics.unlv.edu

²Department of Physics, Guangxi University, Nanning 530004, China

³Department of Astronomy, Nanjing University, Nanjing 210093, China

Draft version October 21, 2018

ABSTRACT

Swift/BAT has detected ~ 200 long-duration GRBs, with redshift measurements for ~ 50 of them. We derive the luminosity function (Φ^{HL}) and the local event rate (ρ_0^{HL}) of the conventional high luminosity (HL) GRBs by using the z -known *Swift* GRBs. Our results are generally consistent with that derived from the *CGRO*/BATSE data. However, the fact that *Swift* detected a low luminosity (LL) GRB, GRB 060218, at $z = 0.033$ within ~ 2 year of operation, together with the previous detection of the nearby GRB 980425, suggests a much higher local rate for these LL-GRBs. We explore the possibility that LL-GRBs as a distinct GRB population from the HL-GRBs. We find that ρ_0^{LL} is $\sim 325_{-177}^{+352} \text{ Gpc}^{-3} \text{ yr}^{-1}$, which is much higher than ρ_0^{HL} ($1.12_{-0.20}^{+0.43} \text{ Gpc}^{-3} \text{ yr}^{-1}$). This rate is $\sim 0.7\%$ of the local Type Ib/c SNe. Our results, together with the finding that less than 10% of Type Ib/c SNe are associated with off-beam GRBs, suggest that LL-GRBs have a beaming factor typically less than 14, or a jet angle typically wider than 31° . The high local GRB rate, the small beaming factor, and low luminosity make the LL-GRBs distinct from the HL-GRBs. Although the current data could not fully rule out the possibility that both HL- and LL-GRBs are the same population, our results suggest that LL-GRBs are likely a unique GRB population and the observed low redshift GRB sample is dominated by the LL-GRBs.

Subject headings: gamma-rays: bursts—gamma-ray: observations—methods: statistical

1. INTRODUCTION

Gamma-ray bursts (GRBs) and supernovae (SNe) are two of the most violent explosions in the Universe. The connection between long duration GRBs and SNe was predicted theoretically (Colgate 1974; Woosley 1993), and has been verified observationally through detecting spectroscopic features of the underlying SNe in GRB 980425/SN 1998bw (Galama et al. 1998; Kulkarni et al. 1998), GRB 030329/SN 2003dh (Stanek et al. 2003; Hjorth et al. 2003), GRB031203/SN 2003lw (Malesani et al. 2004), and GRB 060218/SN 2006aj (Modjaz et al. 2006; Pian et al. 2006; Sollerman et al. 2006; Mirabal et al. 2006; Cobb et al. 2006). In some other cases, red SNe bumps were observed in the late optical afterglow light curves (Bloom et al. 1999, 2002; Della Valle et al. 2003; Fynbo 2004; see a comprehensive sample and references in Zeh et al. 2004). It is long speculated that long GRBs are associated with deaths of massive stars, and hence, SNe (for recent reviews, see Zhang & Mészáros 2004; Piran 2005; Mészáros 2006; Woosley & Bloom 2006). This speculation was broken down by the recent observation of GRB 060614, which is a long, nearby GRB without an accompanied SN (Gehrels et al. 2006; Fynbo et al. 2006; Della Valle et al. 2006; Gal-Yam et al. 2006). Based on its close analogy with the short duration GRB 050724, Zhang et al. (2007a) argued that this event might be also powered by a merger of compact stars. They further suggest that the conventional long *vs.* short GRB classification scheme may be modified as Type I (from mergers) *vs.* Type II (from collapsars) GRBs, and that GRB 060614 belongs to Type I (see also Zhang 2006).

Some authors have attempted to determine the lumi-

osity function (Φ) and the local rate (ρ_0) of long GRBs through fitting the $\log N - \log P$ or V/V_{max} distributions observed by *CGRO*/BATSE (Schmidt 2001; Stern et al. 2002; Lloyd-Ronning et al. 2002; Norris 2002; Guetta et al. 2005) or through simulations (Lloyd-Ronning et al. 2004; Dai & Zhang 2005; Daigne et al. 2006). They consider only high luminosity GRBs (HL-GRBs, with luminosity $L > 10^{49} \text{ erg s}^{-1}$), and generally characterize Φ with a broken power law and obtain $\rho_0^{\text{HL}} \sim 1 \text{ Gpc}^{-3} \text{ yr}^{-1}$ (e.g. Schmidt 2001; Guetta et al. 2004, 2005). Guetta et al. (2004) suggested that by extrapolating the LF of HL GRBs to low-luminosities with a broken power law, one gets $\rho_0^{\text{LL}} \sim 10 \text{ Gpc}^{-3} \text{ yr}^{-1}$ for low redshift GRBs at $z < 0.17$ (GRBs 980425, 031203, and 030329). However, the fact that *Swift* detected GRB(XRF) 060218 at $z = 0.033$ (Mirabal et al. 2006) within ~ 2 years of operation, together with the previous discovery of GRB 980425 at $z = 0.0085$ (Tinney et al. 1998) by BeppoSAX, suggests that the local rate of the GRB 060218-like low luminosity (LL) GRBs (ρ_0^{LL}) is $100 \sim 1000 \text{ Gpc}^{-3} \text{ yr}^{-1}$ (Cobb et al. 2006; Pian et al. 2006; Soderberg et al. 2006b), much higher than ρ_0^{HL} (Schmidt 2001; Stern et al. 2002; Lloyd-Ronning et al. 2002; Norris 2002; Guetta et al. 2004, 2005). This poses a great puzzle about the nature of these LL-GRBs. Are these LL-GRBs from the same population as HL-GRBs (Nakamura 1999; Ioka & Nakamura 2001; Yamazaki et al. 2003; Guetta et al. 2004) or from a sub-energetic GRB population (Kulkarni et al. 1998; Soderberg 2004b; Mazzali et al. 2006; Toma et al. 2006) with a much higher rate than that of the conventional HL-GRBs? In this paper we attempt to address these questions through careful statistical analyses with

the redshift-known *Swift* GRB sample. Throughout the paper $H_0 = 71 \text{ km s}^{-1} \text{ Mpc}^{-1}$, $\Omega_m = 0.3$, and $\Omega_\Lambda = 0.7$ are adopted.

2. DATA AND GRB SAMPLE

The current GRB sample with redshift measurements contains more than 80 GRBs. Since both the observed luminosity and redshift distributions are instrument-dependent (Jakobsson et al. 2006; Zhang et al. 2007b), we use only the long GRBs detected by *Swift* to form a homogeneous sample. *Swift* has detected ~ 200 long bursts during the first 2 years of operation (from December 2004 to November 2006). Among them 47 bursts have redshift measurements. We have excluded GRBs 060505 and 060614 from our sample since they are suggested to be classified as a new type of GRBs (Gehrels et al. 2006; Gal-Yam et al. 2006; Fynbo et al. 2006; Della Valle et al. 2006) or to belong to the short GRB group (Zhang et al. 2007a; Zhang 2006). We therefore obtain a *Swift* HL-GRB sample of 45 bursts. We collect the peak flux and spectral parameters of these GRBs from the literature or GCN Circular reports. It is well known that most broad band GRB spectra are well fitted by the Band function (Band et al. 1993). However, $\sim 80\%$ of the BAT spectra are fitted by a simple power law ($F_\nu \propto \nu^{-\Gamma^{PL}}$) (e.g., Zhang et al. 2007b). This effect is due the narrowness of the BAT band (15-150 keV) and the faintness of the bursts (so that there are not enough counts to perform a Band-spectrum fit. Therefore, the BAT spectra are not the true spectra of the *Swift* GRBs. In order to correct the observed luminosity to a broad band ($1 - 10^4 \text{ keV}$ in this analysis) we have to estimate the parameters of the Band function for each GRB. Zhang et al. (2007b) developed a new method to derive the parameters of the Band function by fitting the observational data with incorporation of the observed spectral hardness ratio. They found a strong correlation between Γ^{PL} derived from the BAT data and E_p of the νf_ν spectrum (see also Zhang et al. 2007a). Sakamoto et al. (2006) independently derived this correlation. We use this method to estimate the parameters of the Band function for the GRBs in our sample, and then correct the observed luminosity to $1 - 10^4 \text{ keV}$ band in the burst rest frame with the k -correction presented by Bloom et al. (2001). The HL-GRB sample has a moderate size, with both a broad luminosity distribution ($L_{iso} = 2 \times 10^{50} \sim 4.6 \times 10^{53} \text{ erg s}^{-1}$) and a broad redshift distribution ($z = 0.55 \sim 6.29$).

3. ANALYSIS METHOD

The number of GRBs per unit time at redshift $z \sim z+dz$ with luminosity $L \sim L+dL$ is given by

$$\frac{dN}{dt dz dL} = \frac{R_{\text{GRB}}(z)}{1+z} \frac{dV(z)}{dz} \Phi(L), \quad (1)$$

where $R_{\text{GRB}}(z)$ is the event rate (in units of $\text{Gpc}^{-3}\text{yr}^{-1}$) as a function of z , $(1+z)^{-1}$ accounts for the cosmological time dilation, and

$$\frac{dV}{dz} = \frac{c}{H_0} \frac{4\pi D_L^2}{(1+z)^2 [\Omega_M(1+z)^3 + \Omega_\Lambda]^{1/2}} \quad (2)$$

¹We have considered the other two star formation models, SF1 and SF3. Our results are not sensitive to the selection of these star formation models since these models are almost the same at low redshifts.

is the comoving volume element at redshift z in a flat Λ CDM universe. We assume that R_{GRB} follows the star formation rate as a function of redshift, and the parameterized star formation model SF2 presented by Porciani & Madau (2001) is used¹,

$$R_{\text{GRB}} = 23\rho_0 \frac{e^{3.4z}}{e^{3.4z} + 22.0}, \quad (3)$$

where ρ_0 is the underlying local GRB rate per unit volume at $z \sim 0$, i.e., $\rho_0 = R_{\text{GRB}}|_{z \sim 0}$. We characterize $\Phi(L)$ as

$$\Phi(L) = \Phi_0 \left[\left(\frac{L}{L_b} \right)^{\alpha_1} + \left(\frac{L}{L_b} \right)^{\alpha_2} \right]^{-1}, \quad (4)$$

where L_b is the break luminosity and Φ_0 is a normalization constant to assure the integral over the luminosity function being equal to unity. Considering an instrument having a flux threshold F_{th} and an average solid angle Ω for the aperture flux, the number of the detected GRBs after an observational period of T should be

$$N = \frac{\Omega T}{4\pi} \int_{L_{\min}}^{L_{\max}} \Phi(L) dL \int_0^{z_{\max}} \frac{R_{\text{GRB}}(z)}{1+z} \frac{dV(z)}{dz} dz, \quad (5)$$

where L_{\max} and L_{\min} are taken as 10^{54} and $10^{45} \text{ erg s}^{-1}$, respectively, and z_{\max} for a given burst with luminosity L is determined by the instrumental flux threshold F_{th} through $F_{\text{th}} = L/4\pi D_L^2(z_{\max})$.

We derive $\Phi(L; \alpha_1, \alpha_2, L_b)$ with the *Swift* GRB sample by using the following procedure. First, we constrain α_1 , α_2 , and L_b by comparing the luminosity and redshift distributions predicted by the model to the observations (1-D Criterion). We calculate the L and z distributions for a given set of the parameters, and then measure the consistency between model predictions and observations with the K-S test (Press et al. 1999). The significance level of the consistency is described by a probability of p_{K-S} . A larger value of p_{K-S} suggests a better consistency (the higher significance level). The consistency for both L and z distributions is therefore measured by $p_{K-S}^T = p_{K-S}^L \times p_{K-S}^z$. Second, we derive ρ_0 for a given Φ by using $N = N^{\text{obs}}$ (N -Criterion). In this analysis we consider only the GRBs detected by Swift/BAT. The aperture solid angle of BAT is 1.33, and the detection numbers of both HL- and LL-GRBs by Swift/BAT in 2 operation years is $N_{\text{HL}}^{\text{obs}} = 200$ and $N_{\text{LL}}^{\text{obs}} = 1$. The sensitivity curve of BAT in the 50-150 keV band (Band 2003) is adopted. Third, we use a 2-dimensional GRB number distributions in the $[\log L, \log(z)]$ -plane to further examine the parameters and evaluate the influence of the observational biases of the sample (2-D Criterion). The 1-D Criterion constrains the parameters with the *clustered* bursts in the sample. The 2-D Criterion, instead, present a self-consistency test with the scattered data points by assuming that the burst distribution in the $[\log L, \log(z)]$ -plane predicted by a reasonable Φ should cover the observational data points at a 3σ confidence level.

4. ARE HL-GRBS AND LL-GRBS THE SAME POPULATION?

We first study the constraints on Φ^{HL} with the the current z -known HL-GRB sample, and then analyze whether or not it can predict the detection rate of LL-GRBs by extrapolating Φ^{HL} down to a luminosity as that of GRBs 980425 and 060218.

4.1. Luminosity Function and Local Rate of HL-GRBs

Following the methodology discussed above, we derive the luminosity function and local rate of HL-GRBs with our z -known HL-GRB sample. Figure 1(a) and (b) show the distribution of p_{K-S}^T in $(\alpha_1^{\text{HL}}, \alpha_2^{\text{HL}})|_{L_b^{\text{HL}}=2.3 \times 10^{52}}$ and $(\alpha_1^{\text{HL}}, L_b^{\text{HL}})|_{\alpha_2^{\text{HL}}=2.3}$ planes, respectively. Our sample includes 44 bursts, and a value of $p_{K-S}^T > 0.05$ marginally suggests the consistency between the model predictions and the observations. Therefore, we show the contours for $p_{K-S}^T > 0.05$ only. From Fig.1 we find that the parameters are convolved. Different combinations of these parameters could make the consistency between both the luminosity and redshift distributions and the observations. Nonetheless, strong constraints on the parameters could be derived from Fig.1. First, the value of α_1^{HL} is required to be smaller than 1.1 (marked by a vertical line in the two panels). Second, L_b^{HL} is correlated with α_1^{HL} . This correlation is roughly described by a function of $\log L_b^{\text{HL}} / (1.2 \pm 0.6) 10^{52} = \alpha_1^{\text{HL}^3}$ [marked by solid and dashed curves in Fig. 1(a)]. Third, α_2^{HL} should be larger than 1.5, and a preferred value from our sample is $2.0 < \alpha_2^{\text{HL}} < 2.6$ and $0.5 < \alpha_1^{\text{HL}} < 0.8$ [with $p_{K-S}^T > 0.15$, marked by an ellipse in Fig. 1(b)].

With these constraints on the parameters we derive the distribution of ρ_0^{HL} through simulations. We take $\alpha_1^{\text{HL}} = 0.65 \pm 0.15$, $\alpha_2^{\text{HL}} = 2.3 \pm 0.3$, and $L_b^{\text{HL}} / 10^{52} = (1.2 \pm 0.6) \times 10^{\alpha_1^{\text{HL}^3}}$. We assume a normal distribution of the errors for α_1^{HL} , α_2^{HL} , and $\log L_b^{\text{HL}}$, and simulate 1000 sets of $(\alpha_1^{\text{HL}}, \alpha_2^{\text{HL}}, \log L_b^{\text{HL}})$. We then calculate ρ_0^{HL} for each set of the parameters with Eq. 5 by taking $N = N_{\text{obs}}^{\text{HL}}$. The distribution of the ρ_0^{HL} together with that of these parameters are shown in Fig. 2. We obtain $\rho_0^{\text{HL}} = 1.12^{+0.43}_{-0.20} \text{ Gpc}^{-3} \text{ yr}^{-1}$ at a 90% confidence level. The 1-dimensional and 2-dimensional distributions of the luminosity and redshift predicted by our model with $\alpha_1 = 0.65$, $\alpha_2 = 2.3$, $L_b = 2.25 \times 10^{52} \text{ erg s}^{-1}$ are shown in Fig. 3. It is found that both the one-D z and L distributions predicted by our model are consistent with the observations, and all the HL-GRBs in the 2-dimensional plane are enclosed in the 3σ region. Both Φ^{HL} and ρ_0^{HL} are consistent with those derived from the BATSE data (e.g. Schmidt 2001; Stern et al. 2002; Guetta et al. 2005) and simulations (e.g. Dai & Zhang 2005; Daigne et al. 2006).

4.2. LL-GRBs as the Low Luminosity End of the HL-GRB Population?

We estimate ρ_0^{LL} with the two detections of GRB 060218 and GRB 980425 from,

$$N = \rho_0^{\text{LL}} V_{z < 0.033} \frac{\Omega^{\text{Bepp}} T^{\text{Bepp}} + \Omega^{\text{Sw}} T^{\text{Sw}}}{4\pi} = 2, \quad (6)$$

²Please note that GRB 060218 shows significant hard-to-soft spectral evolution (Campana et al. 2006; Ghisellini et al. 2006) and the peak energy of its integrated spectrum matches the Amati-relation (Amati et al. 2006). GRB 980425 significantly deviates this relation. Ghisellini et al. (2006) argued that by considering the spectral evolution effect, GRB 980425 may be also consistent with the Amati-relation.

where $V_{z < 0.033} \sim 1.2 \times 10^{-2} \text{ Gpc}^3$ is the volume at $z < 0.033$, $\Omega^{\text{Bepp}} = 0.123$ and $\Omega^{\text{Sw}} = 1.33$ are the solid angles of the GRBM on board *BeppoSAX* and the BAT on board *Swift*, respectively, and $T^{\text{Bepp}} \sim 6$ years and $T^{\text{Sw}} \sim 2$ years (at the time when this paper is written) are the operation periods of the *BeppoSAX* and *Swift*, respectively. We obtain $\rho_0^{\text{LL}} \sim 600 \text{ Gpc}^{-3} \text{ yr}^{-1}$. This is much larger than ρ_0^{HL} derived above (see also Cobb et al. 2006 and Soderberg et al. 2006b). A simple extrapolation of Φ^{HL} derived above to low luminosities cannot account for such a high ρ_0^{LL} (e.g. $\rho_0^{\text{LL}} \sim 10 \text{ Gpc}^{-3} \text{ yr}^{-1}$; Guetta et al. 2004). This rate yields only a Poisson probability of 5.1×10^{-4} for detecting the two events at $z < 0.0331$. In order to argue a same population for both HL and LL GRBs and keep a high ρ_0^{LL} , the only way is to invoke a much larger α_1 than α_1^{HL} derived above. We fix $\alpha_2 = 2.3$, $L_b = 5 \times 10^{52} \text{ erg s}^{-1}$, and $N = 200$, and search for a α_1 value that can yield a local rate as $\sim 600 \text{ Gpc}^{-3} \text{ yr}^{-1}$. We obtain $\alpha_1 \sim 1.6$. The derived one-D and two-D distributions of the redshift and luminosity are shown in Fig.4. One can see that the model predictions are significantly deviated from the observations. The model greatly overpredicts GRBs with $z \sim 1.2$ and $L \sim 3 \times 10^{52} \text{ erg s}^{-1}$. Although this result could not fully rule out the possibility that LL-GRBs are simply the low luminosity end of the HL-GRB population (Guetta et al. 2004), it does disfavor such a possibility. In the above analysis we do not consider the difference of the beaming effects for both HL- and LL-GRBs and the LF cosmological evolution effect. As we discuss below, the LL-GRBs are likely less collimated and are detectable in the nearby universe only.

5. LL-GRBS AS A DISTINCT GRB POPULATION FROM HL-GRBS

As discussed above, the high detection rate of the LL-GRBs motivates us to consider the LL-GRBs as a distinct GRB population from the HL-GRBs. The conventional HL-GRBs generally have a luminosity of $L > 10^{49} \text{ erg s}^{-1}$. We therefore take a preliminary criterion of $L < 10^{49} \text{ erg s}^{-1}$ to select our LL-GRB sample. LL-GRBs are faint. They are only detectable in a small volume of the local universe and a large amount of the population are below the sensitivity threshold of the detector. The observable LL-GRBs with *Swift* are rare events comparable to HL-GRBs. It is unlikely to establish a large sample with the current GRB missions, so it is difficult to investigate Φ^{LL} through fitting its $\log N - \log P$ distribution or through our 1-D Criteria (as is done for the HL-population). We can only roughly constrain the Φ^{LL} and ρ_0^{LL} with a few detections and limits of LL-GRBs. GRBs 980425 and 060218 are two firm detections of LL-GRBs². There are also two other marginal detections for the LL-GRBs, i.e., GRBs 031203 ($z = 0.105$, $L = 3.5 \times 10^{48} \text{ erg s}^{-1}$) and 020903 ($z = 0.25$, Soderberg et al. 2002; $L = 8.3 \times 10^{48} \text{ erg s}^{-1}$).

5.1. Luminosity Function and local Rate

With the four detections and the other constraints from observations we constrain the LF of these LL-GRBs. The luminosity of these LL-GRBs range from $5 \times 10^{46} \text{ erg s}^{-1}$ to $8.3 \times 10^{49} \text{ erg s}^{-1}$. Assuming also a broken power law

LF for the LL-population (similar to eq.[4]), we take L_b around 10^{47} erg s $^{-1}$ and constrain α_1 and α_2 by requiring that the 3σ contour of the 2-D distribution encloses these LL-GRBs. This places constraints on both α_1 and α_2 . In order to make the 3σ contour marginally enclose the nearest burst, GRB 980425, but not over-predict the detection probability at $z < 0.01$, α_1 should be shallow. Similarly, the α_2 is constrained by GRBs 031203 and 020903. Based on these observational constraints we search for α_1^{LL} and α_2^{LL} by taking $L_b^{\text{LL}} = (1.0 \pm 0.3) \times 10^{47}$ erg s $^{-1}$. We find $\alpha_1^{\text{LL}} = 0 \pm 0.5$ and $\alpha_2^{\text{LL}} \sim 3.0 \sim 4.0$ can roughly reflect these constraints. We use the same simulation method as that for HL-GRBs to derive the distribution of ρ_0^{LL} . The parameters are taken as $\alpha_1^{\text{LL}} = 0 \pm 0.5$, $\alpha_2^{\text{LL}} = 3.5 \pm 0.5$, and $L_b^{\text{LL}} = (1.0 \pm 0.3) \times 10^{47}$ erg s $^{-1}$. The distribution of ρ_0^{LL} together with that of these parameters are also shown in Fig. 2. We obtain $\rho_0^{\text{LL}} = 325^{+352}_{-177}$ at a 90% confidence level. The 2-D distribution in the $(\log L, \log z)$ plane is shown Fig. 3. It is found that the LL-GRBs form a distinct “island” from the main “continental” population. The detection rate of the LL-GRBs thus can be explained without over-predicting the HL-GRBs. These results suggest that the current data are consistent with the conjecture that LL-GRBs form a distinct population from HL-GRBs, with a low luminosity and a high local rate. The constrained luminosity functions for both HL and LL populations are displayed in Fig.5(a).

5.2. Beaming factor

Understanding GRB rates has profound implications for understanding the relation between GRBs and Type Ib/c SNe (e.g. Lamb et al. 2005). Compared with the local Ib/c SN rate ($4.8 \times 10^4 \text{ Gpc}^{-3} \text{ yr}^{-1}$; Marzke et al. 1998; Cappellaro, Evans & Turatto 1999; Folkes et al. 1999), the rate of LL-GRBs (on-beam only, not including those beamed away from the Earth) is about $\sim 0.7\%$ of the Type Ib/c SN rate. Most recently, Soderberg et al. (2006a) argued that at most $\sim 10\%$ of Type Ib/c SNe are associated with off-beam LL-GRBs based on their late-time radio observations of 68 local Type Ib/c SNe. This result, combined with our result, suggest that the beaming factor of these LL-GRBs is at most a factor of 14, in contrast to a higher factor (~ 100 , Frail et al. 2001; Zhang et al. 2004; Guetta et al. 2005) for HL-GRBs. This suggests that LL-GRBs are less collimated, with an opening angle typically larger than $\sim 31^\circ$. This is consistent with the observational data of GRB 060218 (Campana et al. 2006; Soderberg et al. 2006b).

6. OBSERVED LOCAL GRB EVENT RATES OF HL-GRBS AND LL-GRBS

The so-called *observed* local GRB event rate ρ^{obs} crucially depends on the luminosity function, the instrument threshold, and a certain redshift to estimate the rate. Figure 5(a) shows the combined Φ of both LL- and HL- GRBs derived from a set of *ordinary* parameters ($\alpha_1^{\text{HL}} = 0.65$, $\alpha_2^{\text{HL}} = 2.3$, $L_b = 1.20 \times 10^{52} \times 10^{\alpha_1^{\text{HL}3}}$ erg s $^{-1}$; $\alpha_1^{\text{LL}} = 0.0$, $\alpha_2^{\text{LL}} = 3.5$, $L_b^{\text{LL}} = 10^{47}$ erg s $^{-1}$) and from two sets of parameters that are roughly taken as the lower limit ($\alpha_1^{\text{HL}} = 0.5$, $\alpha_2^{\text{HL}} = 2.0$, $L_b^{\text{HL}} = 0.6 \times 10^{52} \times 10^{\alpha_1^{\text{HL}3}}$ erg s $^{-1}$; $\alpha_1^{\text{LL}} = -0.5$, $\alpha_2^{\text{LL}} = 4.0$, $L_b^{\text{LL}} = 7 \times 10^{46}$ erg s $^{-1}$) and upper

limit ($\alpha_1^{\text{HL}} = 0.8$, $\alpha_2^{\text{HL}} = 2.6$, $L_b^{\text{HL}} = 1.8 \times 10^{52} \times 10^{\alpha_1^{\text{HL}3}}$ erg s $^{-1}$; $\alpha_1^{\text{LL}} = 0.5$, $\alpha_2^{\text{LL}} = 3.0$, $L_b^{\text{LL}} = 3 \times 10^{47}$ erg s $^{-1}$) of the LF. It is evident that Φ has two distinct components. We calculate the observed GRB event rates for both LL- and HL-GRBs as a function of “enclosing redshift” z_{enc} (i.e. the volume enclosed by this redshift) for the three parameter sets. The results are shown in Fig.5(b). The observed rates of LL-GRBs and HL-GRBs as a function of redshift are significantly different. $\rho_{\text{obs}}^{\text{LL}}$ keeps almost a constant within $z < 0.1$, and drops sharply at $z > 0.1$. At $z \sim 0.2$ $\rho_{\text{obs}}^{\text{LL}}$ is $\sim 10 \text{ Gpc}^{-3} \text{ yr}^{-1}$, which is roughly consistent with that suggested by Guetta et al. (2004). The $\rho_{\text{obs}}^{\text{HL}}$ is also almost constant within $z < 0.1$, but it increases when $z > 0.1$ and peaks at $z \sim 2.5$, being consistent with the observations with *Swift*. Although $\rho_{\text{obs}}^{\text{LL}}(z)$ has a large uncertainty, (e.g. varies by almost two orders of magnitude), Fig.5(b) indicates that the detectable GRB sample within $z < 0.4$ is dominated by the LL-GRBs.

7. DISCUSSION

We have analyzed the luminosity function and local rate of HL-GRBs and extended this analysis to LL-GRBs. We present detailed discussion on our method, data, and analysis results before drawing the conclusions of our analysis.

Ideally, deriving the luminosity function requires a large, unbiased z -known sample. The current GRB sample, however, is still small and suffers from some observational biases. First, the trigger probability of a burst depends on its peak flux. A weaker burst near the instrument threshold has a lower trigger probability. This effect affects the completeness of the sample at a given instrumental threshold. As shown in Fig.3, a gap between the data points and the threshold curve is observed. The gap manifests this bias. Second, the redshift measurements also have biases against weak GRBs (e.g. Bloom 2003). In order to evaluate whether these observational biases could significantly affect our results, we use the 2-D distribution in the $(\log L, \log z)$ plane at 3σ significance level to examine our results. If these biases do not ruinously affect our results, the 3σ contour of the GRB distribution in the $(\log L, \log z)$ plane should enclose the current GRB sample; otherwise, the model should predict many undetected GRBs near the threshold and the 3σ contour cannot cover the scattered data point in the $(\log L, \log z)$ plane. From Fig.3 we find the data points are enclosed by the 3σ contour for the HL-GRBs, suggesting that these observational biases do not significantly affect our results for HL-GRBs. However, the current *Swift* GRB sample with redshift measurements is still small. One prominent issue is whether both the redshift and luminosity distributions derived from the current *Swift* GRB sample represent the true *observed* ones for the threshold of *Swift*. In order to address this issue we plot also the GRBs detected by previous GRB missions in Fig.3. It is found that most of these GRBs are enclosed by the 3σ contour defined with the current *Swift* HL-GRB sample. Two GRBs, 030329 and 040701, are out of the 3σ contour. In order to make a 3σ contour to enclose the two GRBs, we find that the luminosity function should have $\alpha_1 > 1.05$, $\alpha_2 \sim 3.0$, and $L_b \sim 6 \times 10^{52}$ erg s $^{-1}$. We also show that the 3σ contour and the predicted L and z distributions of this luminosity function in Fig.3 (dashed line). It predicts more GRBs with $L \sim 10^{49} - 10^{51}$

erg s⁻¹ (roughly the low luminosity end of the HL-GRBs) than observations by *Swift*. If this is indeed an observational bias for the HL-GRB sample with *Swift*, the true α_1 should be larger than that derived from the current *Swift* GRB sample, say, $\alpha_1 \sim 1$. With such a LF, GRB 020903 is enclosed in the 3σ contour and 031203 also marginally belongs to the HL-GRB group. However, even with such a LF, GRBs 980425 and 060218 are definitely not merged into the HL-GRB group.

Another effective approach to evaluate the biases is to fit the observed $\log N - \log P$ distribution. The current *Swift* sample has only ~ 200 bursts. It still cannot be used for making such a fitting. A sample of ~ 500 bursts with ~ 120 redshift measurements could be obtained by *Swift* in a period of 5 years. Such a sample could refine the constraints on the LF of HL-GRBs by incorporating our approach with the $\log N - \log P$ fitting³.

A cosmological evolution effect may influence the derivation of the luminosity function (e.g. Lloy-Ronning et al. 2002). So far there is no robust evidence of such an evolutionary effect with the GRB sample with spectroscopic redshifts. This effect also does not affect Φ^{LL} , since the LL-GRBs are likely detectable only at low redshifts. It may influence the derivation of Φ^{HL} . A large sample of spectroscopic redshift measurements is required to more robustly evaluate this effect. The current HL-GRB sample is inadequate for this task. Therefore, we do not consider this effect in this analysis. In the future, using a sample established by *Swift* within 5 year operation one may be able to robustly model this effect, and the constraints on the luminosity function of HL-GRBs could be further refined.

Our results tentatively suggest that LL-GRBs are an intrinsically different GRB population, characterized by a high local rate, low luminosity, and small beaming factor comparing to the HL-GRBs. The detectable low redshift GRBs should be dominated by the LL-GRBs. Le & Dermer (2007) draw the similar conclusion through modeling the redshift distribution of the *Swift* GRBs. However, we pointed out that the current data do not conclusively exclude the possibility that only one population of GRBs is responsible for both HL- and LL-GRBs (Guetta et al. 2004).

There are two scenarios to explain the nature of the LL-GRBs. One scenario is that these GRBs are standard HL-GRBs viewed off-axially (e.g. Nakamura et al. 1999; Yamazaki et al. 2003). In order to account for the step-like two-component LF displayed in Fig. 4, the jet must include two distinct components, i.e. a narrow HL component and a very wide LL component. Such a jet configuration is different from the conventional jet-cocoon picture in the standard collapsar model in which the cocoon component is not as broad as 31° (e.g. Zhang et al. 2003). The lack of detection of radio re-brightening in GRB 980425 and GRB 031203 (Soderberg et al. 2004a,b) has also greatly constrained this scenario (Waxman 2004a,b).

The second scenario is that LL-GRBs are intrinsically different from HL-GRBs (e.g. Wang et al. 2000; Soderberg et al. 2004b; Mazzali et al. 2006). Actually, the LL-GRBs as a unique GRB population has been proposed

since the discovery of GRB 980425/SN1998bw with its observed under-luminous, long-lag, simple light curve features (e.g., Soderberg et al. 2004b). Stern et al. (1999) suggested a group of “simple” bursts with peak fluxes near the BATSE trigger threshold. Norris (2002) found that the proportion of long-lag, single-pulse bursts (similar to the three LL-GRBs) within long-duration bursts increases from negligible among bright BATSE bursts to $\sim 50\%$ at the trigger threshold, and their peak flux ~ 2 orders of magnitude lower than that of the brightest bursts. Taken together with the fact that three nearby GRBs, 980425, 031203, and 060218, are long-lag and under-luminous (e.g., Sazonov et al. 2004; Liang et al. 2007), an intuitive speculation of the observed LL-GRBs is that they are probably relatively nearby (e.g., Norris et al. 2005) and their local rate should be much higher than conventional HL-GRBs as we derived in this analysis. This scenario calls for a different type of progenitors (e.g. neutron stars rather than black holes) for LL-GRBs from those of HL-GRBs (e.g. Mazzali et al. 2006; Soderberg et al. 2006b). The abundant multi-wavelength observations of GRB 060218 lead us make a step toward to the nature of this kind of events (Wang & Mészáros 2006; Fan et al. 2006; Dai et al. 2006; Li 2007; Ghisellini et al. 2006, 2007; Wang et al. 2006; Gupta & Zhang 2007; Murase et al. 2006; Amati et al. 2006; Liang et al. 2007). Future detectors more sensitive to *Swift* BAT, e.g. EXIST (Grindley 2006), would detect much more of these events and greatly increase the sample of LL-GRBs.

8. CONCLUSIONS

We have derived the luminosity function and the local rate of the HL-GRBs with the *Swift* z -known GRB sample and explored the possibility that LL-GRBs as a unique GRB population from the HL-GRBs. We find that ρ_0^{LL} is $\sim 325_{-177}^{+352}$ Gpc⁻³ yr⁻¹, which is much higher than ρ_0^{HL} ($1.12_{-0.20}^{+0.43}$ Gpc⁻³ yr⁻¹). This rate is $\sim 0.7\%$ of the local Type Ib/c SNe. Our results, together with the finding that less than 10% of Type Ib/c SNe are associated with off-beam GRBs, suggest that LL-GRBs have a beaming factor typically less than 14, or a jet angle typically wider than 31° . The high local GRB rate, the small beaming factor, and low luminosity make the LL-GRBs distinct from the HL-GRBs. Although the current data could not fully rule out the possibility that both HL- and LL-GRBs are the same population, our results suggest that LL-GRBs are likely a unique GRB population and the observed low redshift GRB sample is dominated by LL-GRBs.

We note that Guetta & Della Valle (2007) reproduce the three main results, i.e., the high local rate of LL-GRBs, HL- and LL-GRBs as two populations, and wide jet opening angle for LL-GRBs, three months after we posted this paper to astro-ph. They also suggest that the possibility of one population for both the HL- and LL-GRBs (Guetta et al. 2004) cannot be convincingly ruled out.

We thank Don Lamb for helpful discussion. This work was supported by NASA under grants NNG05GB67G, NNG05GH92G and NNG05GH91G (EWL, BZ & ZGD),

³The $\log N - \log P$ distribution is sensitive to the instrument threshold. One has to use a sample observed by a given instrument to make such a fit. *CGRO*/BATSE established a large sample and such a fit gives $\alpha_1 = 0.3 \sim 1.0$ and $\alpha_2 \sim 2 \sim 3$ by different authors. This is consistent with our results shown in Fig.1

and the National Natural Science Foundation of China under grants 10463001 (EWL) and 10221001 & 10233010

(ZGD).

REFERENCES

- Amati, L., Della Valle, M., Frontera, F., Malesani, D., et al. 2006, A&A, submitted (astro-ph/0607148).
- Band, D., Matteson, J., Ford, L., Schaefer, B., et al. 1993, ApJ, 413, 281
- Band, D. L. 2003, ApJ, 588, 945
- Bloom, J. S. 2003, AJ, 125, 2865
- Bloom, J. S., Kulkarni, S. R., Djorgovski, S. G., Eichelberger, A. C., et al. 1999, Nature, 401, 453
- Bloom, J. S. et al. 2002, ApJ, 572, L45
- Bloom, J. S., Frail, D. A., & Sari, R. 2001, AJ, 121, 2879
- Campana, S., Mangano, V., Blustin, A. J., Brown, P., Burrows, D. N., et al. 2006, Nature, 442, 1008
- Cappellaro, E., Evans, R., & Turatto, M. 1999, A&A, 351, 459
- Cobb, B. E., Bailyn, C. D., van Dokkum, P. G., & Natarajan, P. 2006, ApJ, 645, L113
- Colgate, S. A. 1974, ApJ, 187, 333
- Dai, X. & Zhang, B. 2005, ApJ, 621, 875
- Dai, Z. G., Zhang, B., & Liang, E. W. 2006, astro-ph/0604510
- Daigne, Frédéric; Rossi, E. M., Mochkovitch, R., 2006, MNRAS, 372, 1034
- Della Valle, M., Malesani, D., Benetti, S., Testa, V., Hamuy, M., et al. 2003, A&A, 406, L33
- Della Valle, M., Chincarini, G., Panagia, N., Tagliaferri, G., et al. 2006, Nature, 444, 1050
- Fan, Y. Z., Piran, T., & Xu, D. 2006, JCAP, 9, 13.
- Folkes, S., Ronen, S., Price, I., Lahav, O., et al. 1999, MNRAS, 308, 459
- Frail, D., Kulkarni, S. R., Sari, R., Djorgovski, S. G., et al. 2001, ApJ, 562, L55
- Fynbo, J. P. U., Watson, D., Thoene, C. C., Sollerman, J., et al. 2006, Nature, 444, 1047
- Fynbo, J. P. U., Sollerman, J., Hjorth, J., Grundahl, F., et al. 2004, ApJ, 609, 962
- Galama, T. J., Briggs, M. S., Wijers, R. A. M., Vreeswijk, P. M., et al. 1998, Nature, 395, 670
- Gal-Yam, A., Fox, D., Price, P., Davis, M., et al. 2006, Nature, 444, 1053
- Gehrels, N., Norris, J. P., Mangano, V., Barthelmy, S. D., et al. 2006, Nature, 444, 1044
- Ghisellini, G., Ghirlanda, G., Mereghetti, S., Bosnjak, Z., et al. 2006, MNRAS, 372, 1699
- Ghisellini, G., Ghirlanda, G., Tavecchio, F. 2007, MNRAS, 375, L36
- Grindley, J. E. 2006, in S. S. Holt, N. Gehrels & J. A. Nousek (eds), AIP Conf. Proc., 836, 631
- Guetta, D., Perna, R., Stella, L., & Vietri, M. 2004, ApJ, 615, L73
- Guetta, D., Piran, T., & Waxman, E. 2005, ApJ, 619, 412
- Guetta, D. & Della Valle, M., 2007, ApJ, in press (astro-ph/0612194).
- Gupta, N. & Zhang, B., Astroparticle Physics, 2007, in press (astro-ph/0606744)
- Hjorth, J., Sollerman, J., Moller, P., Fynbo, J. P. U., et al. 2003, Nature, 423, 847
- Ioka, K., Nakamura, T. 2001, ApJ, 554, L163
- Jakobsson, P., Levan, A., Fynbo, J. P. U., Priddey, R., et al. 2006, A&A, 447, 897
- Kulkarni, S. R., Frail, D. A., Wieringa, M. H., Ekers, R. D., et al. 1998, Nature, 395, 663
- Lamb, D. Q., Donaghy, T. Q. & Graziani, C. 2005, ApJ, 620, 355
- Le, T. & Dermer, C. D. 2007, ApJ, in press (astro-ph/0610043)
- Li, L. X., 2007, MNRAS, 375, 240
- Liang, E. W., Zhang, B. B., Stamatikos, M., Zhang, B., et al. 2007, ApJ, 653, L81
- Lloyd-Ronning N. M., Fryer, C., & Ramirez-Ruiz E. 2002, ApJ, 574, 554
- Lloyd-Ronning, N. M., Dai, X. Y., & Zhang, B. 2004, ApJ, 601, 371
- Mészáros, P. 2006, Rep. on Prog. in Phys. 69, 2259
- Marzke, R. O., da Costa, L. N., Pellegrini, P. S., Willmer, C. N. A., & Geller, M. J. 1998, ApJ, 503, 617
- Mazzali, P. A., Deng, J. S., Nomoto, K., Sauer, D. N., et al. 2006, Nature, 442, 1018
- Malesani, D., Tagliaferri, G., Chincarini, G. Covino, S. et al. 2004, ApJ, 609, L5
- Mirabal, N., Halpern, J. P., An, D., Thorstensen, J. R., & Terndrup, D. M. 2006, ApJ, 643, L99
- Modjaz, M., Stanek, K. Z., Garnavich, P. M., Berlind, P., et al. 2006, ApJ, 645, L21
- Murase, K., Ioka, K., Nagataki, S., Nakamura, T. 2006, ApJ, 651, L5
- Nakamura, T. 1999, ApJ, 522, L101
- Norris, J. P., Bonnell, J. T., Kazanas, D., Scargle, J. D., et al. 2005, ApJ, 627, 324
- Norris, J. P. 2002, ApJ, 579, 386
- Pian, E., Mazzali, P. A., Masetti, N., Ferrero, P., et al. 2006, Nature, 442, 1011
- Piran, T. 2005, Rev. Mod. Phys., 76, 1143
- Porciani, C. & Madau, P. 2001, ApJ, 548, 522
- Press, W. H., et al 1999, Numerical Recipes in Fortran, Cambridge University Press
- Sakamoto, T., et al. 2006, ApJ, submitted
- Sazonov, S. Y., Lutovinov, A. A., Sunyaev, R. A., 2004, Nature, 430, 646
- Schmidt, M. 2001, ApJ, 552, 36
- Soderberg, A. M., et al. 2002, GCN Circ. 1554
- Soderberg, A. M., Frail, D. A., & Wieringa, M. H. 2004a, ApJ, 607, L13
- Soderberg, A. M., Kulkarni, S. R., Berger, E., Fox, D. W., et al. 2004b, Nature, 430, 648
- Soderberg, A. M., Nakar, E., Berger, E., Kulkarni, S. R. 2006a, ApJ, 638, 930
- Soderberg, A. M., Kulkarni, S. R., Nakar, E., Berger, E., et al. 2006b, Nature, 442, 1014
- Sollerman, J., Jaunsen, A. O., Fynbo, J. P. U., Hjorth, J., et al. 2006, A&A, 454, 503
- Stanek, K. Z., Matheson, T., Garnavich, P. M., Martini, P. et al. 2003, ApJ, 591, L17
- Stern, B. E., Atteia J.-L., & Hurley K. 2002, ApJ, 578, 304
- Stern, B. E., Poutanen, J., & Svensson, R. 1999, ApJ, 510, 312
- Tinney, C. 1998, IAUC 6896, 1
- Toma, K., Ioka, K., Sakamoto, T., Nakamura, T. 2007, ApJ, in press (astro-ph/0610867)
- Wang, X. Y. & Mészáros, P., 2006, ApJ, 643, L95
- Wang, X. Y., Dai, Z. G., Lu, T., Wei, D. M., & Huang, Y. F. 2000, A&A, 357, 543
- Wang, X. Y., Li, Z., Waxman, E. & Mészáros, P. 2006, ApJ, submitted (astro-ph/0608033)
- Waxman, E. 2004a, ApJ, 602, 886
- Waxman, E. 2004b, ApJ, 605, L97
- Woosley, S. E. & Bloom, J. 2006, ARA&A, 44, 507
- Woosley, S. E. 1993, ApJ, 405, 273
- Yamazaki, R., Yonetoku, D., & Nakamura, T. 2003, ApJ, 594, L79
- Zeh, A., Klose, S., Hartmann, D. H., et al. 2004, ApJ, 609, 952
- Zhang, B. 2006, Nature, 444, 1010
- Zhang, B., Zhang, B. B., Liang, E. W., Gehrels, N., Burrows, D. N. & Mészáros, P. 2007a, ApJ, 655, L25
- Zhang, B., Liang, E. W., Page, K. L., Grupe, D. et al. 2007b, ApJ, 655, 989
- Zhang, B., & Mészáros, P., 2004, Int. J. Mod. Phys. A, 19, 2385
- Zhang, B., Dai, X., Lloyd-Ronning, N. M. & Mészáros, P. 2004, ApJ, 601, L119
- Zhang, W., Woosley, S. E. & MacFadyen, A. I. 2003, ApJ, 586, 356

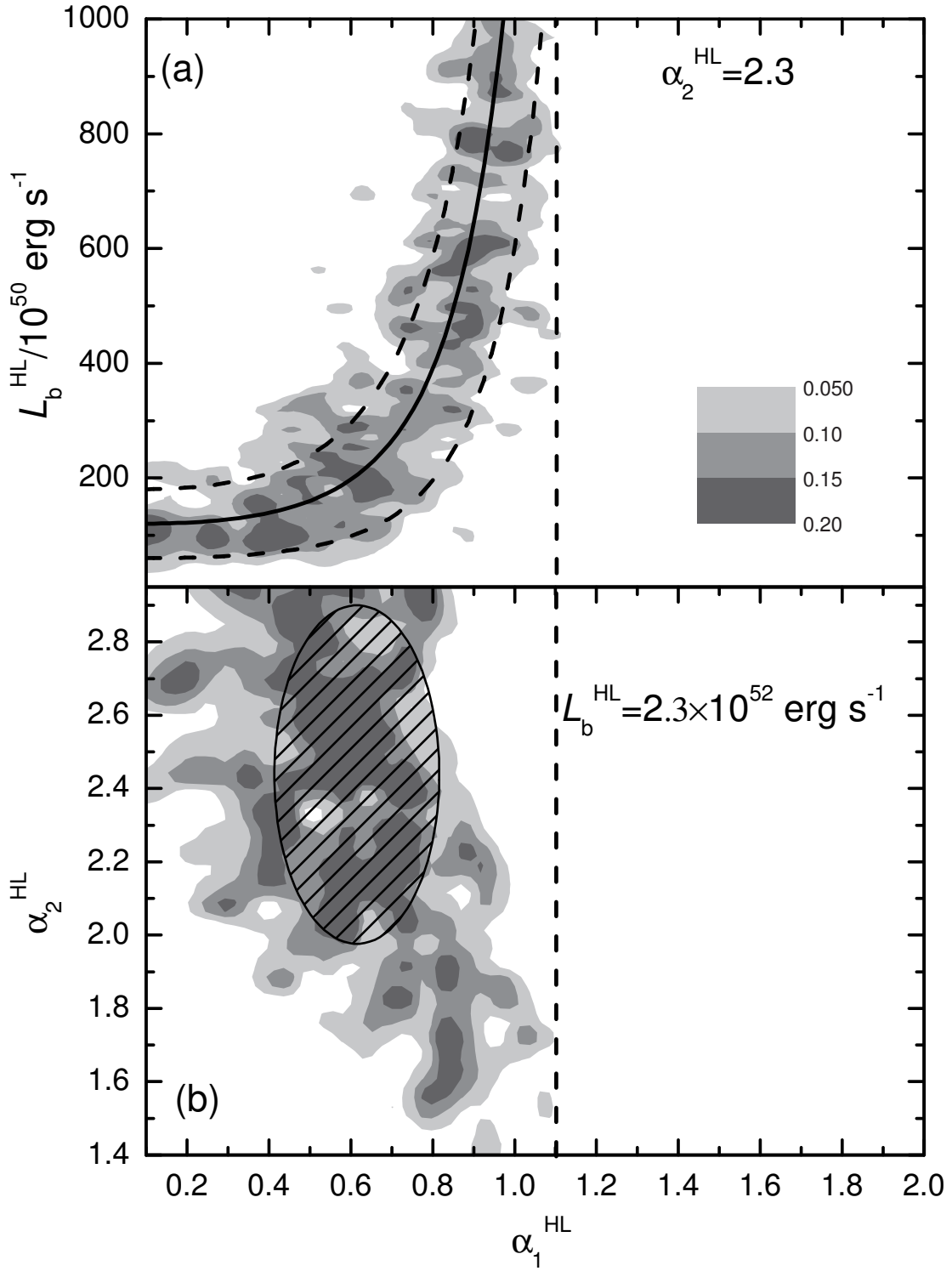


FIG. 1.— Distributions of p_{K-S}^T in the planes of $(\alpha_1^{\text{HL}}, L_b^{\text{HL}})|_{\alpha_2^{\text{HL}}=2.3}$ (panel a) and $(\alpha_1^{\text{HL}}, \alpha_2^{\text{HL}})|_{L_b^{\text{HL}}=2.3 \times 10^{52}}$ (panel b) derived with the current *Swift* HL-GRB sample. The vertical dashed line marks a limit on α_1 . The curves in the panel (a) show the relation and its errors between L_b^{HL} and α_1^{HL} . The ellipse in panel (b) marks the best parameters of α_1^{HL} and α_2^{HL} .

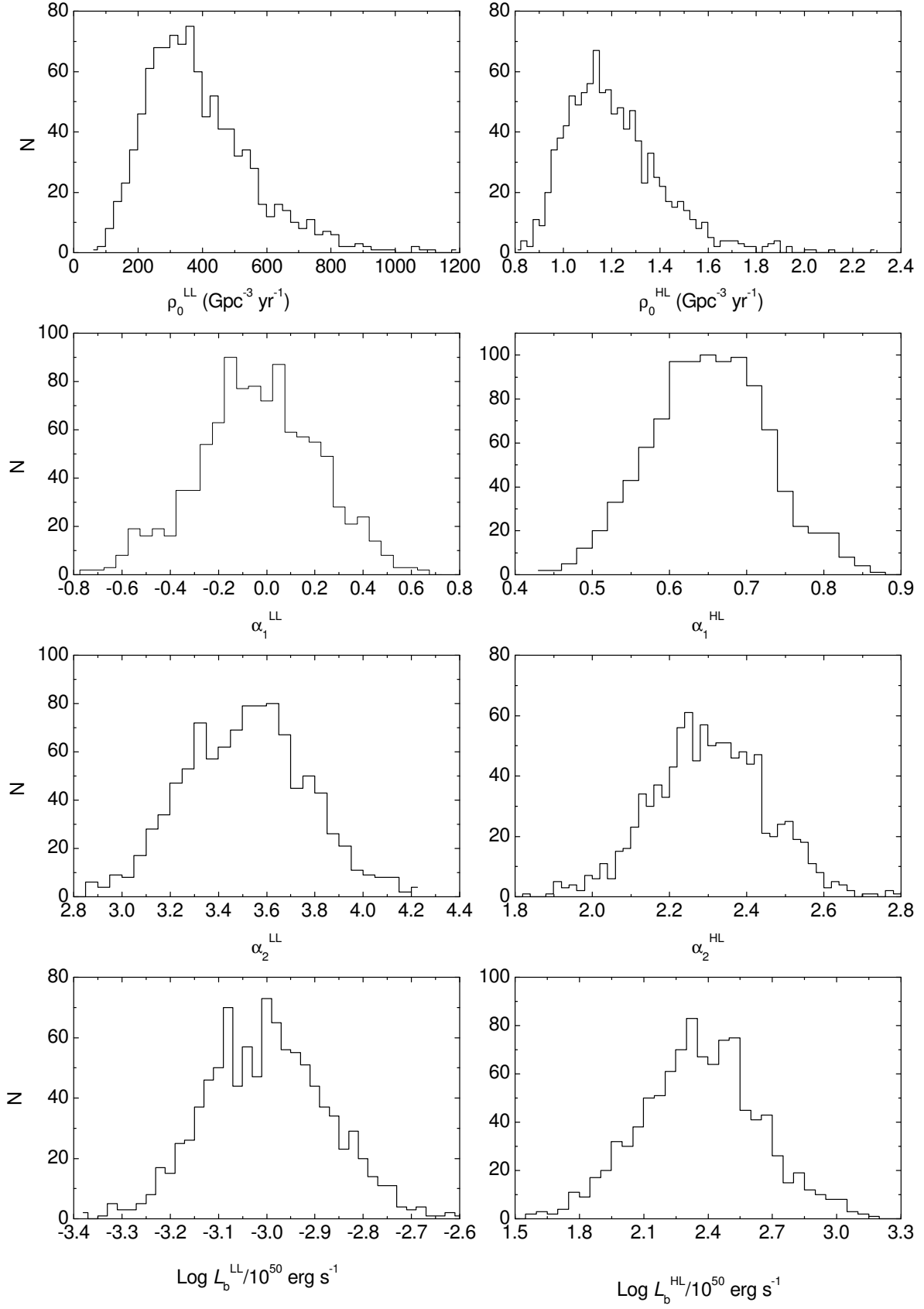


FIG. 2.— Distributions of the GRB local event rates and the parameters of the LFs for LL-GRBs (*left panels*) and HL-GRBs (*right panels*).

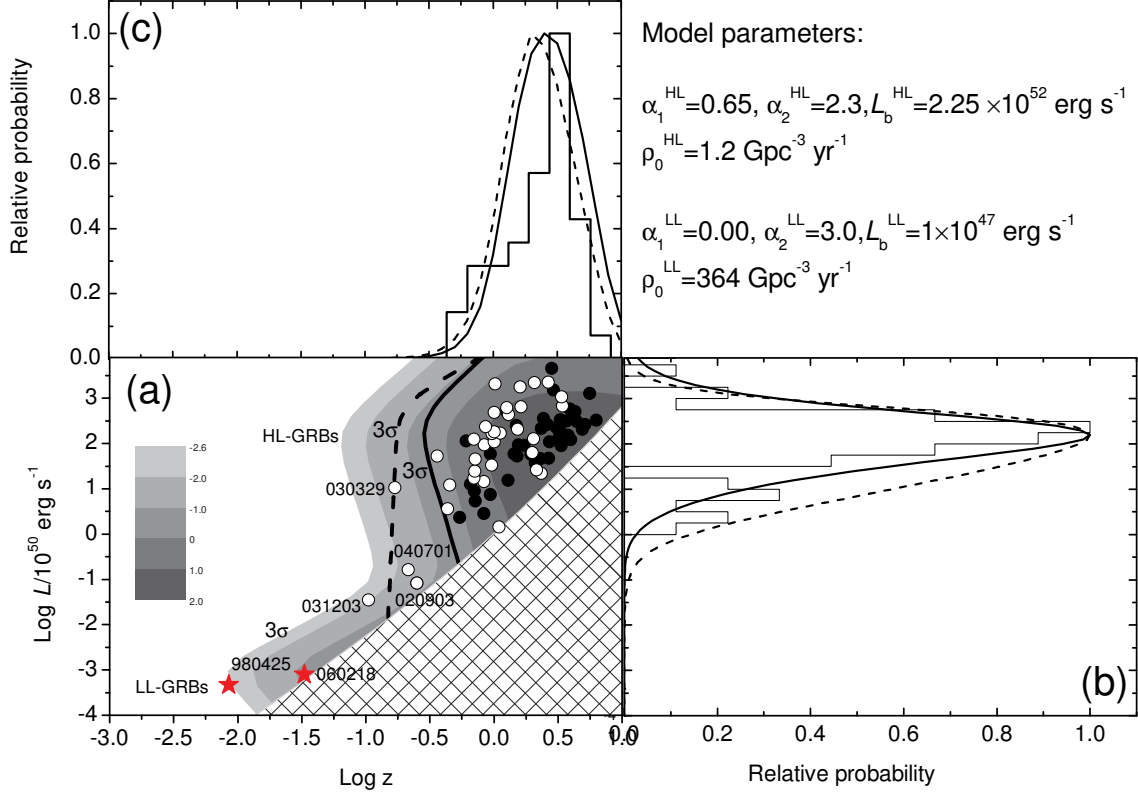


FIG. 3.— Joint contours of the logarithmic GRB detection rate $[\log(dN/dt)]$ distribution in a 2-dimensional (2-d) $[\log L, \log(z)]$ -plane as compared with observational data [panel (a)], assuming that the HL- and LL- GRBs are two distinct populations. The two firm LL-GRBs are denoted by stars, and the *Swift* HL-GRBs are denoted by solid dots. The hatched region marks the limitation of the *Swift*/BAT detectability, where the threshold is derived by using the *Swift*/BAT sensitivity in the 50-150 keV band for a *standard* GRB with $E_p = 200$ keV in the GRB local frame. The bold-faced, solid curves in panel (a) marks the 3σ confidence level of the 2-d distributions for the HL- and LL-GRBs. The comparisons of the observed 1-d distributions of $\log L$ and $\log z$ with the model predictions are presented in panels (b) and (c), respectively. The dashed curve in the panel (a) and the dashed lines in the panels (b) and (c) are, respectively, the 3σ contour of the 2-d distribution and the corresponding 1-d distributions derived from a LF with $\alpha_1^{\text{HL}} = 1.05$, $\alpha_2^{\text{HL}} = 3$, and $L_b^{\text{HL}} = 6 \times 10^{52} \text{ erg s}^{-1}$, which gives a 3σ contour that can enclose all the HL-GRBs observed by *Swift* and pre-*Swift* missions (see §7 in the text).

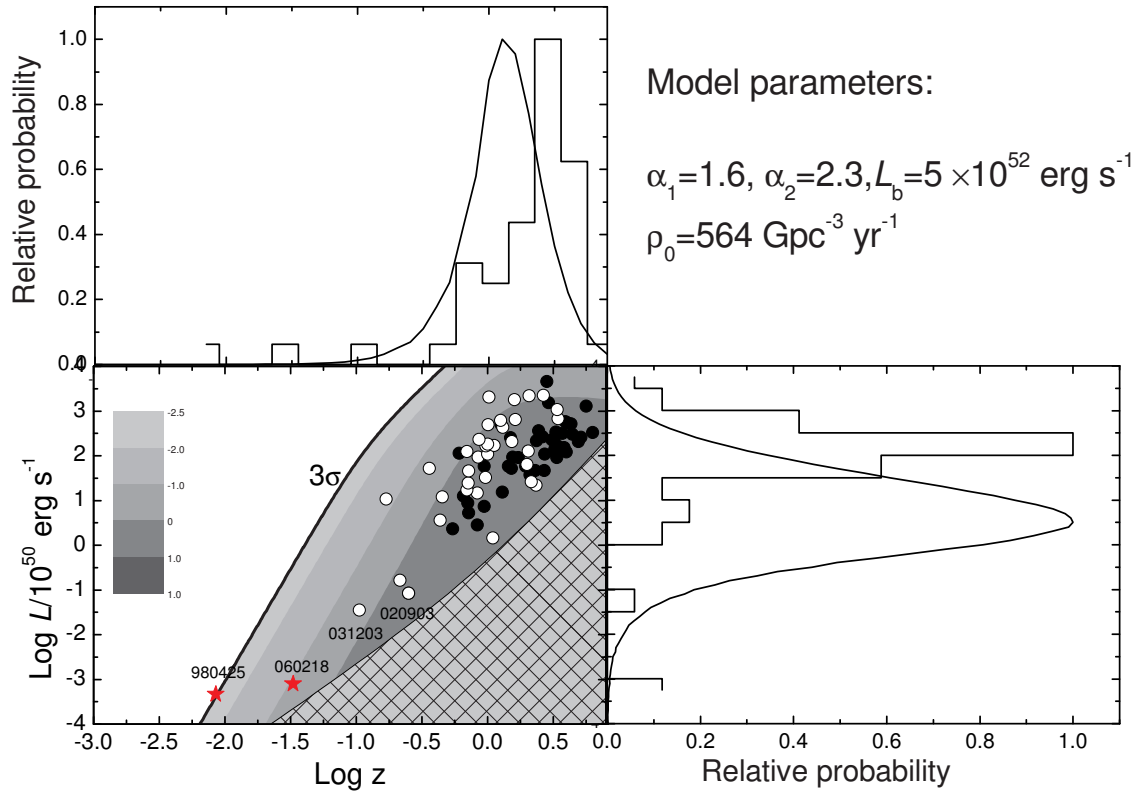


FIG. 4.— Same as Fig.3 but for the case that the HL- and LL- GRBs are assumed to belong to the same population.

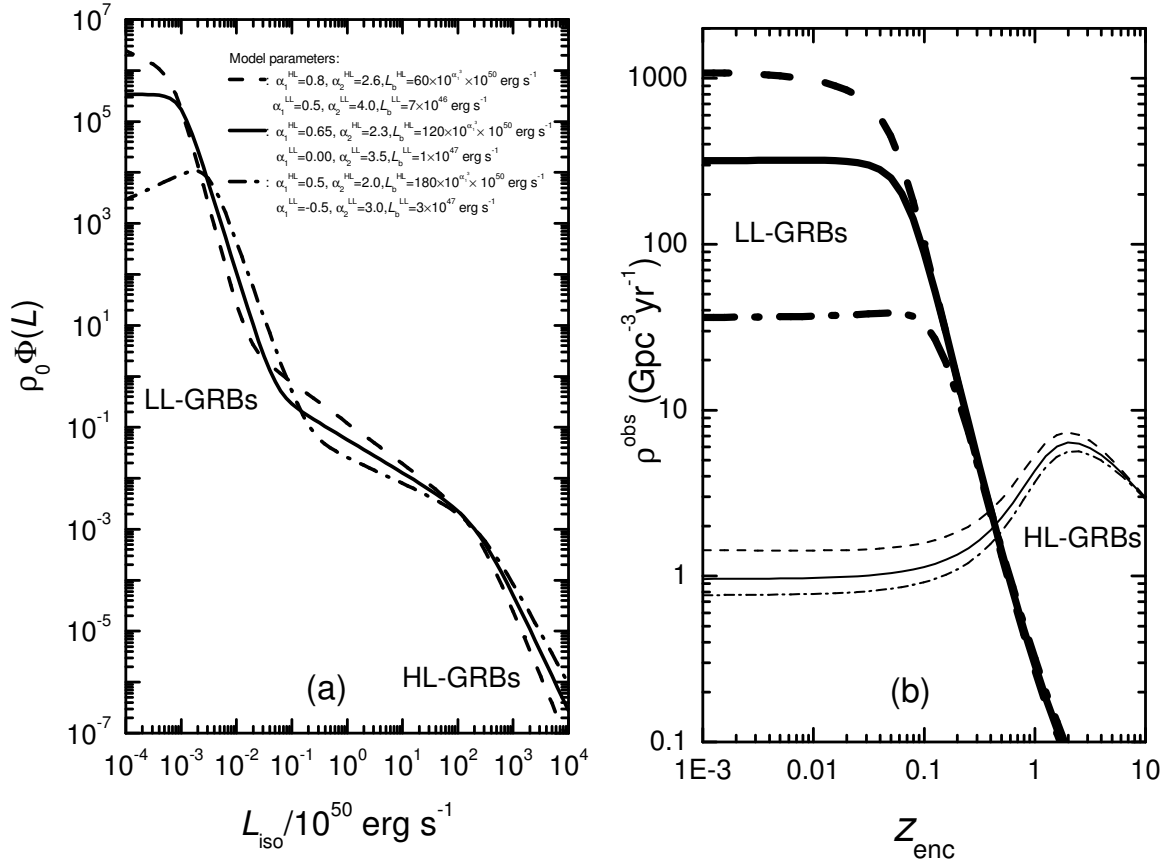


FIG. 5.— *Panel (a)*: The combined LFs of both LL- and HL- GRBs derived from a set of *ordinary* parameters (solid line) and from two sets of parameters that are roughly regarded as the lower (dash-dotted line) and upper (dashed line) limits of the LFs. *Panel (b)*: The observed GRB event rates for both LL- and HL-GRBs as a function of “enclosing redshift” z_{enc} (i.e. the volume enclosed by this redshift) for the three parameter sets shown in panel (a). Same line styles for different models are adopted in both panels.